Visual Cueing Considerations in Nap-of-the-Earth Helicopter Flight by Head-Slaved Helmet-Mounted Displays[1]

Arthur J. Grunwald[2]
NRC Senior Research Associate
Aerospace Human Factors Research Divisions
NASA Ames Research Center
Moffett Field, California, 94035

Silvia Kohn
Faculty of Aerospace Engineering
Technion, Haifa, Israel

ABSTRACT
The Pilot's ability to derive Control-Oriented Visual Field Information from teleoperated Helmet-Mounted displays in Nap-of-the-Earth flight, is investigated. The visual field with these types of displays, commonly used in Apache and Cobra helicopter night operations, originates from a relatively narrow field-of-view Forward Looking Infrared Radiation Camera, gimbal-mounted at the nose of the aircraft and slaved to the pilot's line-of-sight, in order to obtain a wide-angle field-of-regard. Pilots have encountered considerable difficulties in controlling the aircraft by these devices. Experimental simulator results presented here, indicate that part of these difficulties can be attributed to head/camera slaving system phase lags and errors. In the presence of voluntary head rotation, these slaving system imperfections are shown to impair the Control-Oriented Visual Field Information vital in vehicular control, such as the perception of the anticipated flight path or the vehicle yaw rate. Since, in the presence of slaving system imperfections, the pilot will tend to minimize head rotation, the full wide-angle field-of-regard of the line-of-sight slaved Helmet-Mounted Display, is not always fully utilized.

INTRODUCTION
With head-slaved Helmet-Mounted Displays (HMD's), the image of a forward looking camera, such as an Infrared Radiation or a low-light level camera, mounted on a servo-driven gimbals system at the front of the helicopter, is transferred to a miniature helmet mounted Cathode Ray Tube (CRT). By means of collimating optics and a beam splitter, the image is presented to a single eye so that it appears to be superimposed on the visual field at infinity. The camera motions are slaved to the pilot's Line-of-Sight (LOS), by measuring the pilot's head angles in pitch and yaw, and by imparting this information to the camera servo drives. The LOS slaving system of HMD's allows the field-of-regard of the pilot to be extended well beyond the limits of the narrow field-of-view of the HMD's viewing optics. Thus, just by rotation of the head, the pilot is able to cover a field-of-regard of nearly up to 180 deg horizontally, and 90 deg vertically. In addition, in most cases, the camera is positioned such that its view is not obstructed by the aircraft body. This allows the pilot to view areas which are usually blocked out by the cockpit. This wide-angle coverage is very essential in Nap-of-the-Earth (NOE) flight, both for vehicular control by allowing the pilot the necessary spatial orientation with respect to terrain and obstacles, and for the detection and location of targets or mission threats in military missions, or survivors in rescue missions.

Although the LOS slaved HMD apparently solves the problem of providing a wide-angle coverage for the given narrow field-of-view of the HMD optics, vehicular control with such systems is still very difficult, and demands high pilot proficiency and work load. Part of these difficulties can be attributed the fact that the viewpoint of the camera is displaced with respect to the actual eye position. In the presence of fast vehicle pitch or yaw rotations this might result in misjudged vehicle motions. Furthermore, for a camera mounted in front of the pilot, near objects will appear larger than they actually are.

Additional difficulties arise from the relatively narrow field-of-view of the HMD's viewing optics, resulting from practical limitations on the miniature CRT face-plate dimensions, the dimensions and shape of the beam splitter and its minimal safe distance to the pilot's eye, and the collimating system design. Thus, essential parts of the pilot's peripheral vision are missing, which may result in impaired motion perception.

Considerable difficulties are also encountered in the interpretation of FLIR images, which are basically different from visible light images, usually resulting in misjudged object size and impaired depth perception.

The head-slaved HMD resembles a viewing aperture without optics, attached to the pilot's head, which allows him to frame-in different areas of the outside world by rotation of the head. The HMD one-to-one slaving system and the deliberate choice of a

unity image magnification, attempt to give the pilot the illusion of viewing a natural visual scene through such an aperture. For an ideal slaving system, the viewed image would appear to be part of an inertially stable background. However, slaving system errors will be experienced by the pilot as undesired shifts of the displayed visual field with respect to the true "natural" visual field. The effect of these shifts is two-fold: (1) they will alter the optical flow-field pattern and result in incorrect estimation of the self-motion; and (2) the visually estimated self-motion will be different from the motion estimated by vestibular cues. This might lead to visuo-vestibular conflicts or motion sickness, Oman [1]. In coordinated fixed-wing aircraft flight, the velocity vector will coincide with the vehicle longitudinal axis and the pilot can infer the direction of motion from vehicle-based references, by means of his kinesthetic sense of straight ahead. However, in helicopter flight, the direction of motion can deviate substantially from the vehicle axis. Thus helicopter control in NOE flight, is susceptible in particular to these slaving system imperfections, since the Control-Oriented Information has to be derived entirely from the visual field, and can not rely on vehicle based references.

This paper deals with the basic experiments for understanding the Visual Field Information in HMD's Displays, and investigates how this information is affected by slaving system imperfections. Two types of experiments were carried out: (1) a flight path estimation experiment, in which the pilot had to judge the anticipated vehicle path, while being flown passively in a straight or curved horizontal path over flat textured terrain, and (2) a simulated Nap-of-the-Earth flight experiment, in which the pilot subject had to fly actively through a winding canyon, in the presence of purposefully induced head motions.

VISUAL FLOW FIELD CUES

A detailed geometrical analysis of visual flow field cues in horizontal flight over textured flat terrain, is given in Ref. [2]. In this paper we shall suffice with a brief qualitative description.

The visual flow field resulting from an observer's self-motion, is given by the time derivative of a set of line-of-sight (LOS) vectors extending from the pilot's eye to conspicuous points in the visual field (texture points). The flow field is the pattern traced by the intersection of these LOS vectors with a unity sphere about the observer's head. These traces are commonly referred to as the "streamer" pattern. For straight or constantly curved motion at fixed velocity and altitude above a flat surface, the flow field is constant.

Flow field cues in straight flight

The horizontal situation for straight and level flight is shown in Fig. 1a. The center of gravity of the vehicle moves along a straight path in the direction of the velocity vector $\underline{V}$, while the longitudinal vehicle axis is x_b is rotated with respect to $\underline{V}$ by the crabbing angle β. The camera axis x_h is rotated with respect to the vehicle axis by the angle ψ_h. The corresponding streamer pattern is shown in Fig. 1b. The horizontal and vertical axes in Fig. 1b are the viewing azimuth angle and elevation angle, (the latter is measured positive in upwards direction).

For straight flight the streamer pattern appears to expand from a common focal point on the horizon, point F, see Fig. 1b. This point has often been called the "focus of expansion", Gibson [3-5]. The straight vehicle path is defined by the set of points which do not have an azimuth LOS rate component, see solid line. This is also the streamer that is apparently vertical, i.e. perpendicular to the horizon or to the base of the HMD image frame, for zero vehicle roll angle. The dotted box in Fig. 1a indicates the area of the visual field, viewed by the HMD. The center of this box, H, indicates the camera axis x_h and coincides with the pilot's direction of gaze. The vehicle longitudinal axis x_b is indicated by point C. The head angle ψ_h is the angle between H and C, and the vehicle crabbing angle β is the angle between F and C. In case the crabbing angle β is zero, F and C coincide and the direction of motion is presented to the pilot implicitly by kinesthetic head position cues. However, for arbitrary large angles of β this is not the case, and the direction of motion has to be derived solely from the streamer pattern.

Fig. 1b. indicates that the focal point F is not necessarily located within the HMD field-of-view. In this case, the direction of motion is derived by estimating the point where the streamers line segments, visible within the HMD viewing area, would intersect. It has been shown in Ref. [2] that the detectability of the direction of motion depends on the local expansion, which is defined as the derivative of the streamer direction with respect to the azimuth angle. This local expansion is shown to be proportional to the viewing distance to the texture point, measured along the LOS. It therefore appears, that the direction of motion is most easily perceived in the far visual field, where the local expansion is the largest. However, the streamer pattern can only be perceived when the magnitude of the LOS rates are above a certain threshold. It is shown in Ref. [2] that these LOS rates are inverse proportional to the squared viewing distance. A possible mechanism for estimating the straight vehicle path is to extrapolate the focal point from converging streamer segments, located within an area of the visual field, at the farthest

viewing distance at which the streamer direction can still be detected, and at which the local expansion is the largest. It is clear that when this area is not within the HMD field-of-view, the pilot will have to shift his gaze to a different area of the visual field.

Flow field cues in curved flight

The horizontal situation for steady curved flight over flat terrain is shown in Fig. 2a. The instantaneous velocity vector is $\underline{V}$, and β is again the crabbing angle. However, the actual vehicle path is a circle with radius R, tangential to $\underline{V}$ and with its center at point M. The corresponding streamer pattern

is shown in Fig. 2b. This pattern shows a converging, curved set of lines, and a common focal point on the horizon no longer exists. The curved vehicle path is the dashed, central line in the bundle. The vehicle path is defined by the streamer which, for very close viewing ranges, will have a zero azimuth LOS rate component and which tend to be tangential to the velocity vector (solid vertical line). This tangent is again apparently vertical, i.e. perpendicular to the horizon or to the base of the HMD image frame, for zero vehicle roll angle.
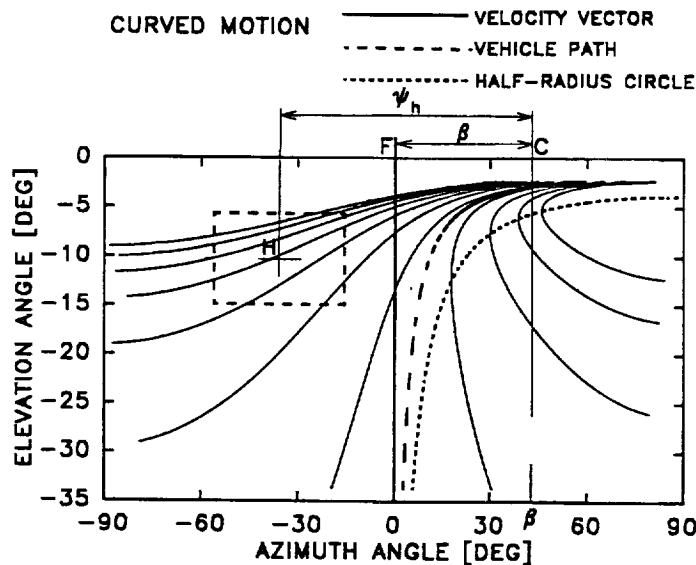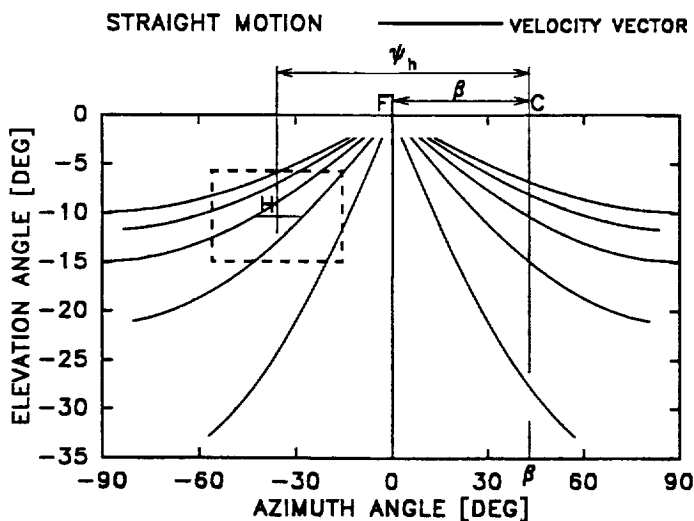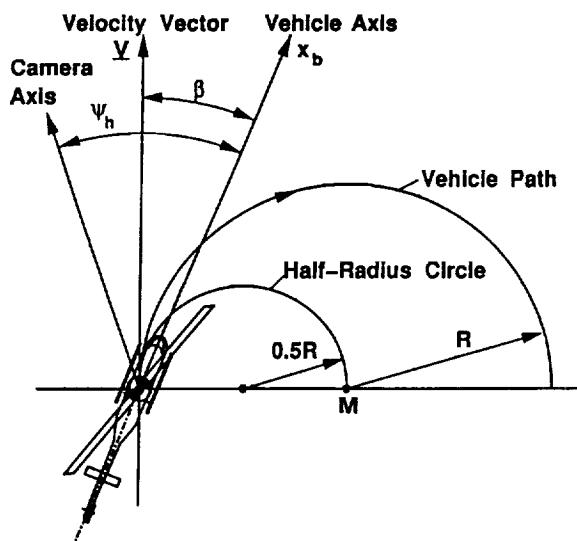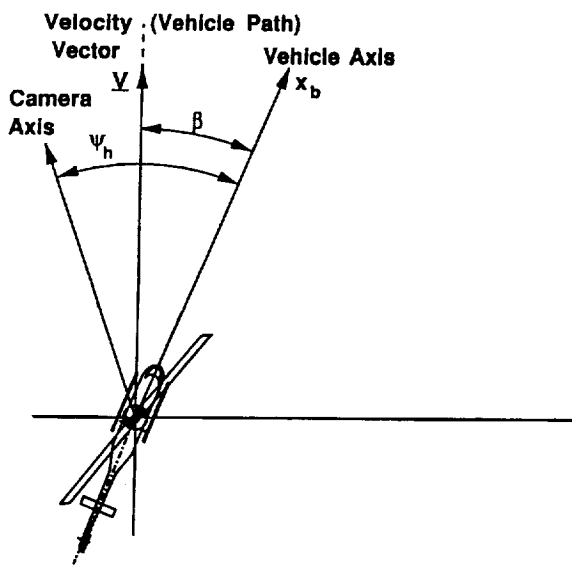
Figure 1. (a) Horizontal Situation for Straight and Level Flight; (b) Streamer Pattern for Straight and Level Flight over Flat Textured Terrain

Figure 2. (a) Horizontal Situation for Curved Level Flight; (b) Streamer Pattern for Curved Level Flight over Flat Textured Terrain

317

It is of interest to consider points in the visual field, which do not have an azimuth LOS rate component. It is shown in Ref. [2] that the locus of these points is formed by the circle, tangential to $\underline{V}$ and with radius 0.5R , hereafter referred to as the "half-radius circle". This locus is shown in Fig. 2b as the dotted line. For viewing distances D<<R, the azimuth angle of a point on the vehicle path is about half way in between the azimuth angle of the velocity vector and of a point on the half-radius circle.

A possible mechanism for estimating a point on the vehicle path, would look for the azimuth angle of the area at viewing distance D, with a zero azimuth LOS rate component, (on the half-radius circle). In addition, the mechanism would estimate the azimuth of the velocity vector by looking, at very close distances, for points with a zero azimuth LOS rate component. It would then estimate the azimuth of a point on the vehicle path at distance D to be half way in between the two angles. A shortcoming of this

mechanism is that it will break down when the point on the half-radius circle is outside the field-of-view.

Another possible mechanism would be to look for continuity of motion between points in the visual field. It would select a set of points which belong to a certain section of the streamer, by following the motion of a texture point over a given interval of time. It would then find the correspondence between streamer sections which would add up to the central streamer, i.e. the one of which the azimuth LOS rate component for close viewing distances, is zero, or, alternatively, the streamer which tends to be tangential to the apparent vertical. This would involve viewing near as well as far areas of the visual field.

The dotted box in Fig. 2b. again shows the area of the visual field, viewed by the HMD. Regardless of the mechanism used, active head motions of the pilot will be required, since the estimation of the curved
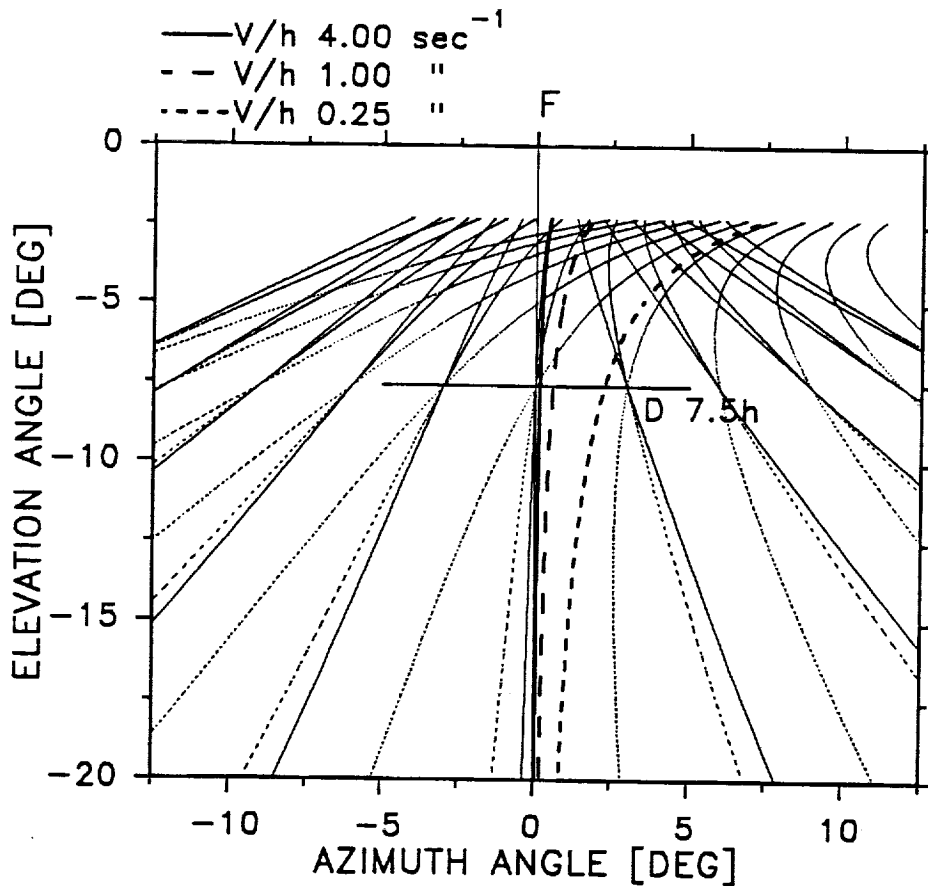

Figure 3: Streamer Pattern "Bending" Effect Resulting From Line-of-Sight Slaving System Lags

318

vehicle path is based on different areas of the visual field, which involve either points on the half-radius circle or points nearby.

Flow field cues in helmet mounted displays

As mentioned before, for an observer in straight or steady curved level flight, a stationary streamer pattern is obtained. Under natural, unconstrained viewing conditions, the streamer pattern and consequently the ability to estimate the vehicle path, will not be affected by voluntary head rotations. This can be attributed to the visuo-ocular reflex, which will inertially stabilize the eye line-of-sight with respect to the viewed background. In this situation, changes in the pattern only result from changes in self-motion parameters. However, the viewing conditions for LOS slaved HMD's differs from natural unconstrained conditions in two ways: (1) the narrow viewing aperture and (2) slaving system imperfections. Due to the narrow viewing aperture, areas essential for estimating the vehicle path might not be in view. Attempts of the pilot to acquire the information might require quick scans of different areas of the visual field, resulting in rapid head motions. However, due to the frame-of-reference effect caused by the narrow viewing aperture, the observer might experience an apparent yaw motion in opposite direction of the voluntary head rotation, Boff [6]. This illusion is caused by strong edge rate effects of image elements passing the edge of the HMD image frame during rotation. The smaller the reference frame, the stronger the effect.

Slaving system imperfections are detrimental in particular in perceiving self-motion information from the visual field. Random tracking errors, scaling errors, or phase lags will result in undesired shifts of the displayed visual field with respect to the true "natural" visual field. These undesired image shifts will make the viewed visual scene appear to move with respect to an inertially stable background. The negative effects of this apparent motion are twofold: (1) Since, during voluntary head rotation, the eye LOS is stabilized with respect to inertial space, the parasitic image shifts will alter the visual field information. (2) The self-motion estimated from the shifted visual field is in conflict with the vestibular signals. This visuo-vestibular conflict might cause motion sickness or disorientation. The following example demonstrates the effect of parasitic image shifts due to LOS slaving system servo lags, on the visual field information contents.

Consider the LOS slaving system to be a second-order system with an natural frequency of ω_n=94.3 rad/s (15 Hz) and with a damping factor of ζ=0.707. Consider the head yaw rotation to be sinusoidal with amplitude A deg and frequency ω rad/s. It is easily shown that for ω<<ω_n the image shift rate amplitude

s is given by: $s=2\zeta A\omega^2/\omega_n$ deg/s.

For example, for A=10 deg and ω=1.0 rad/s the image shift rate amplitude is s=0.15 deg/s. This parasitic yaw rate will add a constant azimuth component to all LOS vector rates. For an observer in straight motion the parasitic yaw rate will make the expanding pattern appear to "bend" momentarily, just as if the observer were in curved motion. It is clear that the larger the ratio between parasitic yaw rate and LOS rate, the larger the "bending" effect. Therefore the negative effects of servo lags are noticed in particular for low self-motion velocities. Fig. 3 shows examples of this "bending" effect, for A=10 deg and ω=1.0 rad/s, for various velocities. Both the velocity V and the viewing distance D are expressed in units of the height h above the terrain. For V/h ratios of 0.25 s and 4.0 s, the angular errors introduced by the bending effect at viewing distance D=7.5h are 2.26 deg and 0.14 deg, respectively.

EXPERIMENTAL PROGRAM

Experimental setup

The visual scene was generated at a Silicon Graphics IRIS 4D 50/GT work station. The pilot subject was seated in a general aviation simulator cabin, wearing an operational flight helmet, on which a Hughes Aircraft miniature CRT with beam splitter and collimating optics was mounted. The monochromatic image, of aperture 22.8 deg horizontally and 18.4 deg vertically, was presented to the subject's left eye only. The right eye was uncovered, viewing the low-light level cockpit background, normally present in night helicopter missions. No outside view or panel mounted display images were presented. A Polhemus head tracking system was used to measure the angular orientation of the head. The measured yaw, pitch and roll head angles were send to the graphics work station, and used for generating the image corresponding with the subject's line-of-sight. Although the Polhemus was sampling at 30 Hz, the image was updated at about 15 Hz. Thus, the system roughly simulated a line-of-sight slaving system with a bandwidth of 15 Hz. Pilot controls included a two-axis high-precision strain gauge operated side-arm controller with response buttons.

Flight path estimation experiment

Each trial represented the situation of passively being flown over nominally flat terrain at height h, either in a straight or constantly curved, level motion pattern. The terrain consisted of a field of randomly placed poles with constant density and with no visible alignment. The average distance between the poles was 1.17 units of h, and their average height was 0.25h. Both the vehicle velocity vector $\underline{V}$, and the vehicle

longitudinal axis x_b were parallel to the ground plane. The vehicle axis was deviating from the velocity vector V by the crabbing angle β, and the curved path was tangential to $\underline{V}$. In order to conserve computational resources and realize an update rate of 15 Hz, the field was not drawn beyond a viewing distance of D=15h.

The subjects initiated an experimental trial by pressing a response button, after which the visual field became visible from an initially blank screen. For each trial the side slip (crabbing) angle β and/or the path curvature radius R were uncorrelated and chosen randomly. A marker was visible in the visual field at viewing distance D, in the direction of gaze, consisting of a circular base of diameter 0.625 h placed in the ground plane with a vertical pole at its center of height 0.125 h. The marker remained at the center of the HMD image, and the subjects could change the marker azimuth just by turning their head. It should be noted that through appropriate geometrical transformations, the marker was kept at all times perpendicular to the ground plane and at a fixed viewing distance D, regardless of head pitch and roll. The subjects were asked to place the marker on the estimated flight path. They were instructed to do this

intuitively, as quickly as possible and to acknowledge their choice by pressing a response button. During the training runs, after each trial, a dotted line was displayed for two additional seconds, indicating the true flight path.

Three types of experiments were conducted: (1) Straight and level flight in the presence of a constant side slip angle β, chosen from a uniformly distributed random set, ranging from -45 to +45 deg. (2) Steady curved and level flight with zero side slip, where the path curvature radius was chosen from a uniformly distributed random set ranging from 15h to 40h and where the curvature could be to the left or to the right with equal probability, and (3) Steady curved and level flight in the presence of side slip, with the curvature chosen as in (2) and with the side slip angle β chosen from an uncorrelated uniformly distributed random set, ranging from -14 to +14 deg.

The relevant parameters investigated were: the velocity-to-height ratio and the viewing distance. Five velocity-to-height ratios were chosen, ranging from 0.25s to 4s. Two viewing distances were chosen, D=7.5h for the far field, and D=3.0h for the near field.

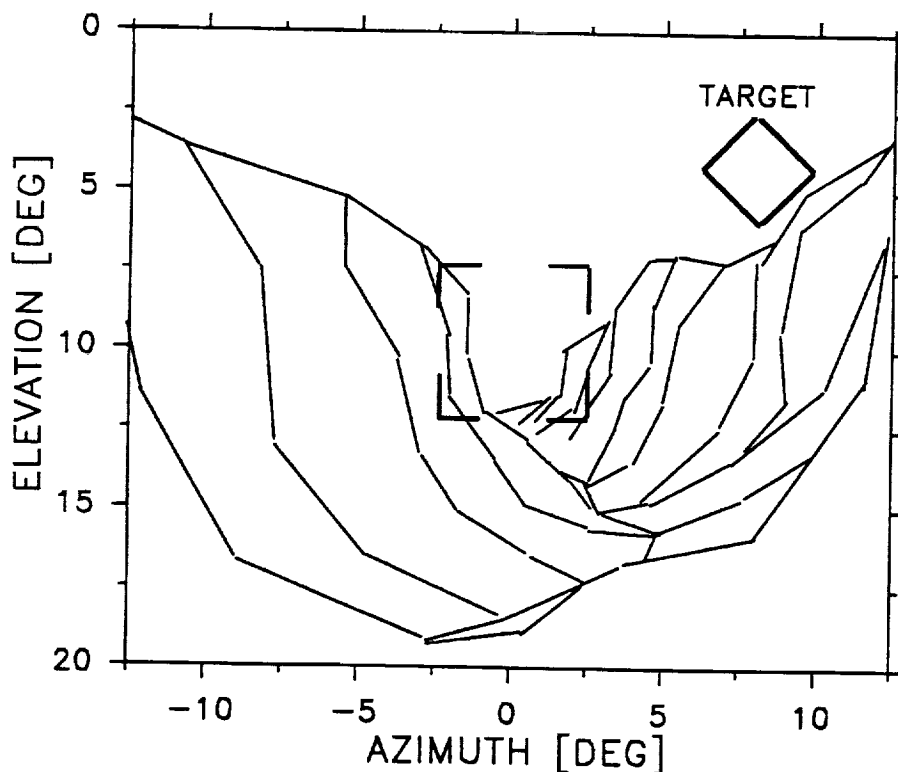
Figure 4: Image of the Randomly Curved Canyon used in the Simulated NOE Flight Experiments

Simulated NOE flight experiment

This experiment simulated the task of actively flying a control-augmented H-19 helicopter through a V-shaped randomly curved canyon, shown in Fig. 4. The horizontal canyon path, and the vertical path profile were generated by passing band-limited white noise processes through a series of shaping filters. The horizontal and vertical path correlation length was about 1500 ft. Two trajectory shapes were considered: a "moderately" curved trajectory with maximum horizontal curvature radii of 500 ft and a strongly curved trajectory with maximum radii of 250 ft. For each run, lasting 180 s, a different random path was generated. The canyon was formed by randomly shaped cross sections spaced 30 ft apart and interconnected by monochrome, solidly drawn polygons of randomly different brightness, simulating a FLIR image. The subjects were instructed to follow the canyon while staying as close as possible to its base without hitting the sides.

Deliberate head rotation was introduced by a secondary task. At random intervals, a diamond-shaped target appeared at a location, fixed with respect to the canyon, see Fig. 4. The target became first visible at a viewing range of 550 ft and disappeared at 300 ft. The subject had to lock his line-of-sight on the target, by bringing it within a 5.7 by 5.7 deg tick mark area in the center of the image. After a successful lock-on, the target and tick marks disappeared. During each run a total of 15 targets were presented. The target locations were chosen such that they involved considerable head rotation, in addition to the rotation needed for following the canyon.

Subject training and experimental procedure

Eight male and one female subject, all of them Technion Aerospace undergraduate students, participated in the experiment. Subject age was between 19 and 24. Subject training for the vehicle path estimation experiments included several one-hour training sessions. After that each subject carried out a series of runs for each one of the three experiments (straight, curved, curved with side slip, in this order). Each series included a number of configurations, each of which was repeated four times and addressed in a random fashion. Each configuration consisted of a set of 20 consecutive trials, each of which was initiated by the subject by pressing a response button. Each trial lasted for about 2-8 seconds, depending on the time needed by the subject to estimate the direction of motion. About 8 one-hour sessions were needed for each subject to finish the experimental program.

Training for the simulated NOE flight experiment required several one hour sessions. Production included simulation runs of 180 s duration, repeated 5 times for each subject and for each configuration. Subject motivation was enhanced by a reward system based on competition.

Experimental measurements

In the flight-path estimation task, for each trial in a set, the error in azimuth angle between the true and estimated location of a point on the flight path at viewing distance D, were recorded, together with the time needed to make the estimate. The upper limit on the estimation time was 8 seconds, after which the run was terminated and marked as a failed run. In addition, the head activity was recorded in terms of the standard deviation of the head yaw angle and yaw angle rate.

For each set of 20 trials, the average and the standard deviation of the estimation error and estimation time, were computed. Since the average of the estimation error was found to be almost zero, i.e. no preference for an error in left or in right direction existed, the standard deviation of the estimation error was adopted as the representative estimation error score of each set. For the estimation time, the average of the set was taken as the representative score.

Performance scores for the NOE flight experiments included the power of the deviation from the bottom of the canyon, standard deviations of head activity, stick activity, vehicle roll and roll rate and the average time needed to lock the line-of-sight on the target.

EXPERIMENTAL RESULTS

Flight path estimation task

Effect of the velocity-to-height ratio:

Figs. 5-8 show the various performance scores as a function of the V/h ratio, for the three motion patterns. For straight motion, (dotted line) the estimation error score strongly decreases with V/h, both for the "far" viewing distance of D/h=7.5h (Fig. 5a) and for the "near" viewing distance of D/h=3.0h (Fig. 5b). In contrast, the downslope of the curves for curved motion and curved motion with side slip, is considerably less. For the near viewing distance the curves are even sloping upwards (Fig 5b). Furthermore, the curves for straight motion for the estimation time and the head yaw rate activity are markedly above the ones for the curved motion patterns, see Figs. 6a,b. This indicates that the subjects probably used a different strategy in the straight motion task. The curves for the head yaw angle and yaw angle rate activity show pronounced and consistent upward slopes, Figs. 7 and 8. This effect can be attributed to the LOS slaving system imperfections, discussed in Section 2.4. The smaller V/h, the stronger the "bending" of the streamer pattern
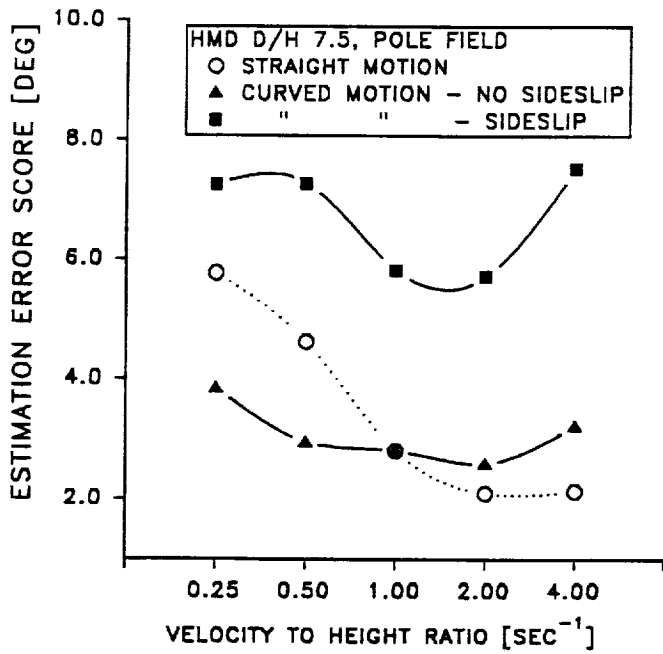
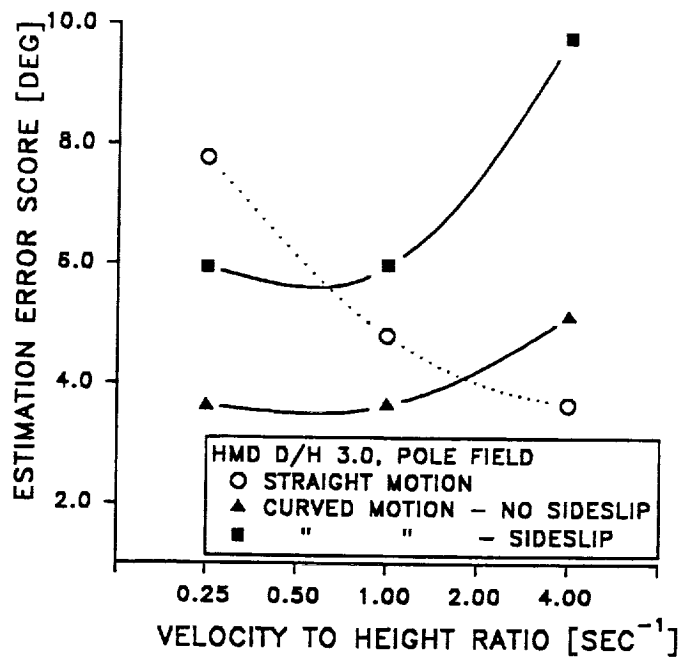**Figure 5a.** Estimation Error Score for D=7.5h
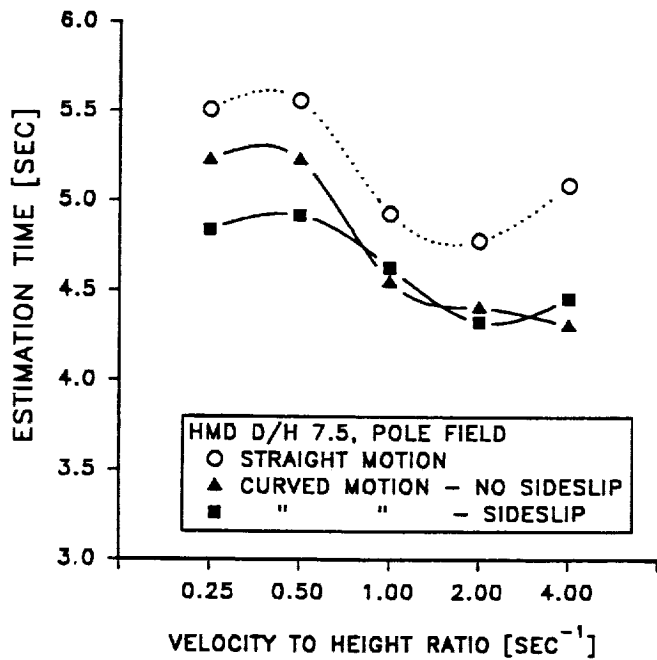

Figure 5b. Estimation Error Score for D=3.0h

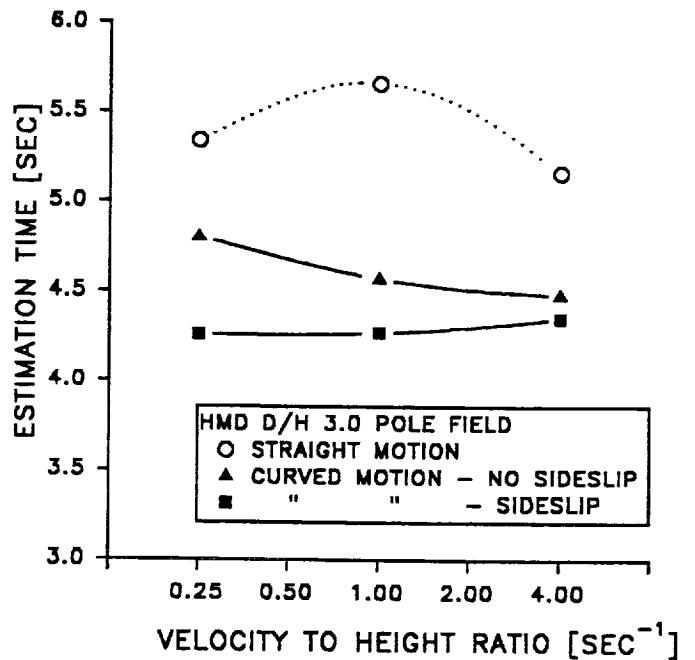**Figure 6a.** Estimation Time for D=7.5h

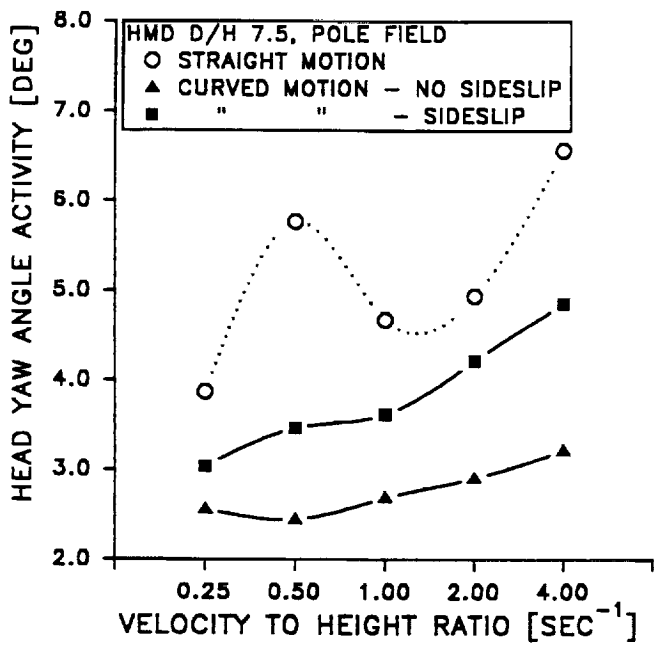**Figure 6b.** Estimation Time for D=3.0h

Figure 7a. Head Yaw Angle Activity for D=7.5h

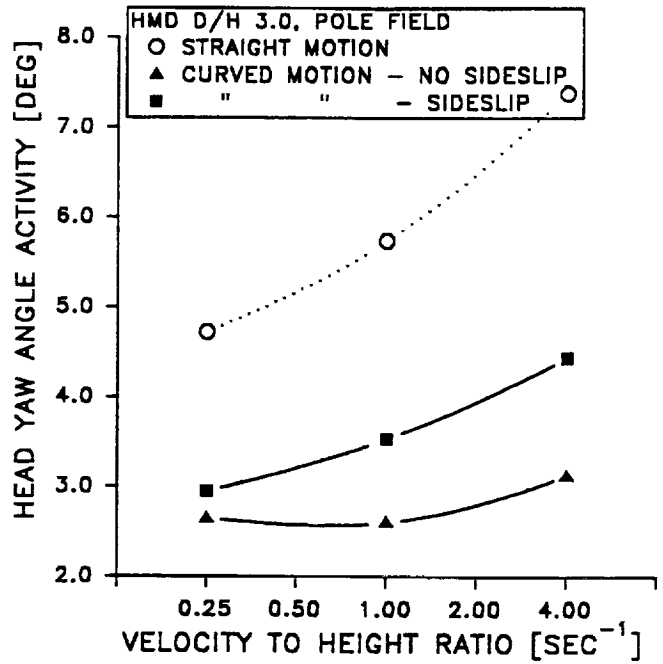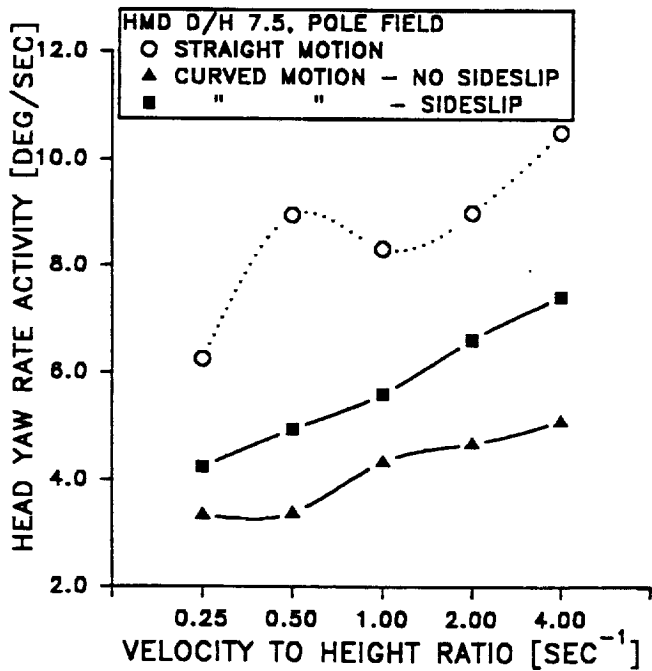**Figure 7b.** Head Yaw Angle Activity for D=3.0h

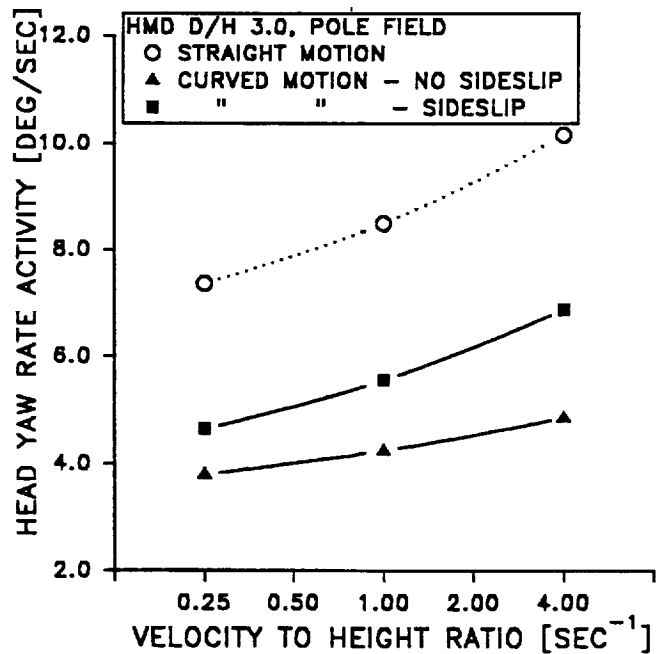**Figure 8a.** Head Yaw Rate Activity for D=7.5h

Figure 8b. Head Yaw Rate Activity for D=3.0h

Figure 9a. Effect of Reduced Field-of-View and LOS Slaving Lags on Estimation Error Score

Figure 9c. Effect of Reduced Field-of-View and LOS Slaving Lags on Head Yaw Angle Activity

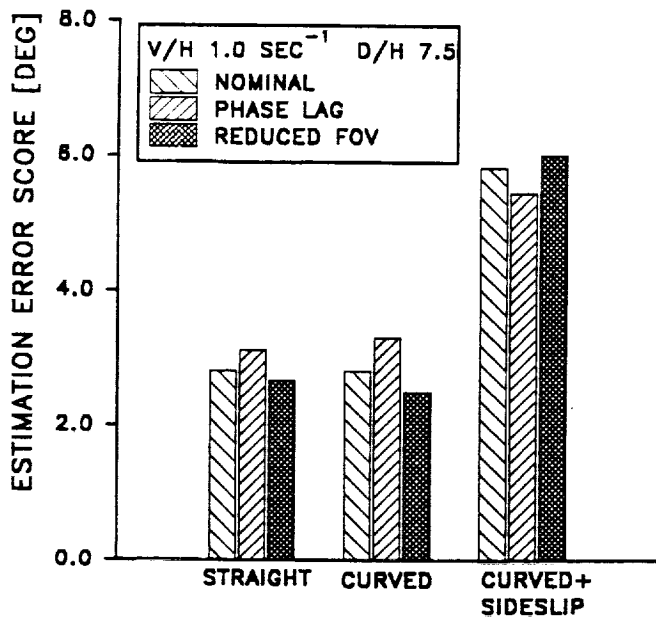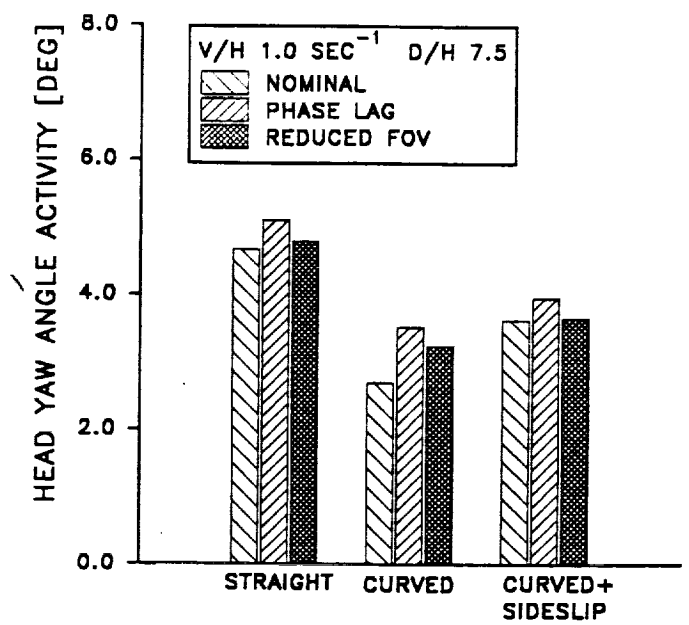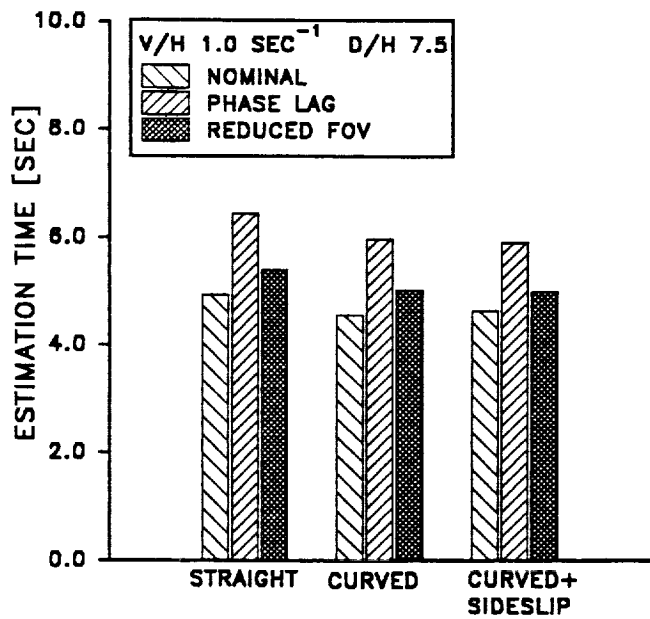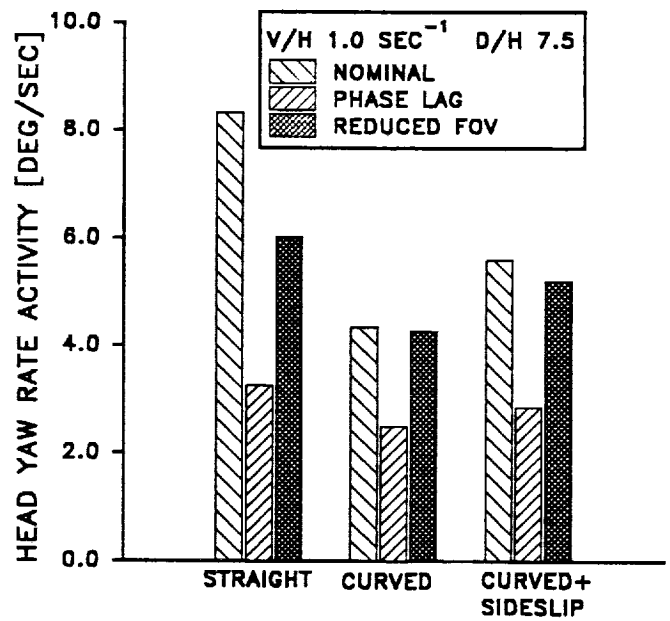**Figure 9b.** Effect of Reduced Field-of-View and LOS Slaving Lags on Estimation Time

Figure 9d. Effect of Reduced Field-of-View and LOS Slaving Lags on Head Yaw Rate Activity

324

during head rotation resulting from slaving system lags, and the less accurate the perception of the streamer direction. This is detrimental in particular in the straight motion task, in which the streamer "bending" makes it almost impossible to find the apparent vertical streamer. As a result, for small velocities subjects will minimize their head rotation, estimates will take longer and estimation errors will be larger. This explains the strong downward slope of the estimation error curve for straight motion, as compared to the more flat curves for curved motion, see Fig. 5a.

Strategy differences between straight and curved tasks are apparent when considering that the subjects are expecting a straight expanding motion pattern in the straight task. Thus, bending effects due to slaving system lags will be identified immediately, and estimates are made only at moments at which the head is stationary. The subjects might have employed a "null measurement" method, in which a sequence of correcting steps is made aimed at placing the apparent vertical streamer at the center. In contrast, in the curved task the subjects might have employed a "deflection measurement" method in which the vehicle path is found intuitively, more or less in an open manner, triggered by the amount of streamer "bending" in the field. Consequently, estimation times and head yaw activity are much larger for the straight task.

Effect of side slip on curved motion:
The estimation error score curves for motion with and without side slip have similar characteristics, i.e. for the far viewing distance a minimum at V/h=1.0 s (Fig. 5a), and for the near viewing distance similar up slopes, (Fig.5b). This up slope might be due to motion "blurring" effects, which prevent the subject from making accurate estimates on the streamer pattern direction. However, the error score curve for motion with side slip is on the average about 3 deg above the one for motion without side slip. This was expected, since in the first case, in the process of estimating the vehicle path, the observer has to derive the direction of motion from the near visual field, whereas in the latter case the direction of motion is at zero azimuth. This direction is presented to him implicitly by kinesthetic head position cues. The increased difficulty to estimate the vehicle path in the presence of side slip is also noticed in the higher head yaw angle and yaw angle rate activity, see Figs. 7 and 8.

Effect of the viewing distance:
A comparison of the curves of Figs. 5a and 5b shows that the near viewing distance yields generally larger estimation errors than the far distance. This might result from the smaller local expansion in the near field. The difference is large in particular for high V/h ratios, probably as a result of image blurring. In contrast, the head yaw rate activity shown in Fig. 8a,b for the near and far viewing distance were found to be very similar. It would be expected that the near field, with its higher LOS rates, would allow larger head rotation, since less streamer "bending" will occur. However, the negative effect of the "bending" will be stronger, due to the smaller local expansion. Therefore, the subjects will still minimize their head rotation for low V/h and for the near viewing distance.

Effect of reduced field-of-view:
The results for an HMD field-of-view reduced to 13.7 deg horizontally and 11.0 deg vertically (40% reduction), are shown in Fig. 9. Contrary to what was expected, estimation errors for all three motion patterns were about the same as for the nominal viewing situation, Fig 9a. However, estimation times were slightly higher (by 9%), and head yaw rate activity lower (by 15%), in particular for straight motion, Fig 9b,c. This indicates that although the reduced field-of-view did not affect estimation accuracy, the subjects might have reduced their head yaw rates due to increased edge rate effects. On the other hand, as expected, the reduced field-of-view demanded slightly more headmotions, as seen in the 6.5% increase in head yaw angle activity

Effect of LOS slaving system lags:
A first-order slaving system lag with a time constant of 0.5 s was introduced. Although the phase lag yielded an only 4% higher error score as compared to the nominal viewing situation, the head yaw rate activity was markedly smaller (by 53%) and, consequently, the estimation time higher (by 30%), see Fig. 9. This clearly demonstrates that slaving system phase lags primarily constrain the subject from making fast head motions, they require from him to make more corrections (14% larger head yaw angle activity), and they result in longer estimation times.

Simulated NOE flight task
Results for the NOE flight task are summarized in Table I. For flight without target capture secondary task, the increase in path curvature has its primary effect on the tracking performance (a 65% increase in tracking error score). The increased path curvature is also strongly noticed in the 31% larger head yaw angle rate. Thus, the high-curvature canyon demands more head activity, which, in the presence of inherent LOS slaving system lags, adversely affects tracking performance. As expected, the increased curvature also yields larger control activity and vehicle roll motions.

The effect of adding the target capture secondary task to the vehicular control task is strongly noticed both in the markedly higher tracking error and in the larger head yaw rates (tracking error scores increase by

Table 1. Simulated NOE Flight Experiment

	Without Target Task		With Target Task	
	Low Curva- ture	High Curva- ture	Low Curva- ture	High Curva- ture
Tracking Error [ft^2]	390.1	643.9	1168.6	1072.5
Head Yaw rate [deg/s]	3.2	4.2	7.4	8.4
Comm. Roll rate [deg/s]	25.7	27.7	27.2	29.1
Comm. Pitch rate [deg/s]	2.6	3.1	3.2	3.7
Vehicle Roll Angle [deg]	7.5	9.4	8.8	10.7
Vehicle Roll Rate [deg/s]	15.6	16.7	16.3	17.5
Target Cap- ture Time [s]	-	-	1.48	1.94
% Missed Targets/Run			6.6	13.0

116% and head yaw rates by 113%). In contrast, control activity and vehicle roll activity increase only slightly. The high correlation between head yaw activity and tracking errors, again demonstrate that head rotation, in excess to the amount needed for the vehicular control task, negatively affects performance. As expected, due to increased main task difficulty, the high-curvature canyon resulted in a 31% higher average target capture time and yielded twice as much missed targets.

Although in this experiment the head rotation is artificially and purposefully induced, similar performance degradation is expected to occur, when the pilot voluntarily moves his head in search of targets or mission threats. Consequently, for HMD's subjected to line-of-sight slaving system lags, the pilot will tend to reduce his head rotation to the minimum required for carrying out the vehicular control task. However, under these conditions, the wide-angle coverage of the line-of-sight slaving system will not be fully utilized and target search performance and spatial orientation will be seriously impaired.

Summary of results

1. The experimental results have clearly shown that line-of-sight slaving system imperfections in HMD's seriously impair the pilot's ability to derive Control-Oriented Information from the visual field. Since, under these conditions, the pilot will tend to minimize head rotations, the wide-angle coverage provided by the slaving system, will not be utilized and search performance and spatial orientation will be impaired.

2. Canyon following performance was found to deteriorate with increased head rotation, either when introduced in a "natural manner" through a higher path curvature, or when induced purposefully by using the target capture secondary task.

3. The vehicle path estimation accuracy and head yaw rate activity generally increase with the V/h ratio. Due to the larger "local expansion" the far viewing distances yield more accurate estimates than close distances. However, due to blurring effects, close distance estimates no longer improve with V/h.

4. The flight path for curved motion is considerably more difficult to estimate than for straight motion, since it relies on the entire streamer pattern rather than on local field estimates. Since in curved flight the near as well as the far field is used, the estimates are less accurate and improve less with increasing V/h ratio.

DISCUSSION

The display system discussed in this paper can be classified as a virtual environment display. Head-mounted displays have become a vital component of virtual environments, which attempt to give the operator the illusion of being physically present in a remotely existing or synthetically generated world. Frequently this objective is achieved by fully immerging the operator in the visual scene by completely blocking out the direct view of the outside world and by presenting the operator with a stereo image of the environment, which is derived either from a remotely located stereo camera pair or computer generated. Although state-of-the-art miniature display technology and computer generated image techniques enable to display images of high quality, detail and authenticity, most system fail to provide the operator with the confidence to move around freely without the fear of stumbling or falling.

The main findings in this paper are valid for this general class of displays as well. While designers of virtual environments are devoting considerable attention to picture contents, quality and detail, the dynamic aspects are often neglected. Detrimental

factors are insufficient update rates, too large time delays due to time-consuming signal communication or highly band limited camera slaving systems. Other factors are inaccurate head position measurements and a lack of rigidity between the display and the head. While these displays may be adequate for a seated person in a near-static environment, in the presence of slow head motions, they often fall short in situations in which self-motion estimation is essential, such as walking, running or controlling a vehicle. Since correct motion estimation from visual cues is only possible when the illusion of an inertially stable background is preserved, deviations induced by system lags or slaving system errors, will result in estimation errors in the self-motion variables. Furthermore, for the person immerged in the environment, the visual cues will be in conflict with the vestibular ones, resulting in disorientation, loss of balance or even motion sickness.

The display, discussed in this paper provides only "partial immersion" since the outside world remains directly visible both to the uncovered eye and to the covered one through the beam-splitter. This arrangement allows the pilot to maintain direct visual contact with the outside world in case of HMD system failures, or for scanning the cockpit instruments. Part of the task difficulty can be attributed to this dichoptic viewing situation, in which the pilot has to switch his attention consciously between the two eyes.

Future research effort should be devoted to exploring ways to eliminate the need for maintaining direct visual contact with the outside world by incorporating all necessary information in a stereoscopic, full immersion display. This might require integrating the present cockpit panel information in the HMD image, and the use of superimposed display symbology, such as a vehicle path trace, a vehicle axis or velocity vector symbol. This superimposed symbology would serve in compensating for the lack of peripheral vision resulting from the narrow HMD field-of-view. Engineering efforts should be devoted primarily to solving the display-to-head rigidity problem, minimizing slaving system errors and enlarging the effective HMD field-of-view.

REFERENCES
1. Oman, C.M., "Sensory Conflict in Motion Sickness: an Observer Theory Approach," in: Pictorial Communication in Virtual and Real Environments, Eds. Ellis, S.R., Kaiser, M.K. and Grunwald, A.J., Taylor and Francis, 1991.

2. Grunwald, A.J., Kohn, S. and Merhav, S.J., "Visual Field Information in Nap-of-the-Earth Flight by Teleoperated Helmet-Mounted Displays," SPIE/SPSE Symposium on Electronic Imaging: Science and Technology, Feb. 24 - March 1, 1991, San Jose, Ca., Paper No, 1456-17, 1991.

3. Gibson, J.J., "The Perception of the Visual World," Houghton Mifflin, Boston, Mass., 1950.

4. Gibson, J.J., Olum, P. and Rosenblatt, F., "Parallax and Perspective During Aircraft Landings," American Journal of Psychology, Vol.68, 1955, pp.372-385.

5. Gibson, J.J., Visually Controlled Locomotion and Visual Orientation in Animals," British Journal of Psychology, Vol.49, 1958, pp.182-194.

6 Boff, K.R., Kaufman, L. and Thomas, J.P., "Handbook of Perception and Human Performance," Vol. 1, Wiley N.Y., 1986, page 16-18, pages 17-18 to 17-20.